

## OPTICAL BEHAVIOUR OF YTTRIUM DOPED NICKEL-MAGNESIUM-CADMIUM FERRITE PREPARED BY SOL-GEL AUTOCOMBUSTION METHOD

R.B. BHISE<sup>1</sup> & S.M. RATHOD<sup>2</sup>

<sup>1</sup>Department of Physics, B. J. College, Ale, Tal: Junnar, Pune, India

<sup>1</sup>Science College, SRTM University, Nanded, India

<sup>2</sup>Nanomaterials and Laser Research Laboratory, Abasaheb Garware College, Pune, India

### ABSTRACT

The present work represents, the Yttrium doped  $\text{Ni}_{0.4}\text{Mg}_{0.4}\text{Cd}_{0.2}\text{Fe}_{2-y}\text{O}_4$  Nanoferrites (where  $y = 0.025$  to  $0.125$ ) synthesized using sol-gel autocombustion method. The structural and optical properties were studied using XRD, FTIR and UV-Visible spectroscopy for the prepared samples. The XRD pattern shows that the structure of prepared nanoparticles is spinel with average grain size lies in the range between 17 to 25 nm. Lattice parameter was found to increases with Zn concentration and this may be due to the larger ionic radius of the  $\text{Y}^{3+}$  ion. FTIR spectroscopy confirmed the formation of spinel ferrite and showed the characteristics absorption bands around 554, 1058, 1384, 1600, 2919, 3434 and  $3855\text{ cm}^{-1}$ . The energy band gap was calculated for samples with different ratio and average band gap energy was found to be 4.0743 eV. The substitution was resulted in slight increased in the lattice constant and that sequentially may lead to the slightly increased in the energy gap. Also found that it is in the range of semiconductor materials.

**KEYWORDS:** Sol-Gel Autocombustion Method, Ferrite Nanoparticles, Optical Properties and XRD

**Received:** Dec 06, 2016; **Accepted:** Jan 05, 2017; **Published:** Jan 12, 2017; **Paper Id.:** IJNAFEB20171

### INTRODUCTION

Nanotechnology is the combination of the branches of science such as engineering, physics, chemical engineering, medical biology and the applications of nanomaterials<sup>1</sup>; which are applicable in electromechanical devices, optical devices, magnetic devices, and tissue engineering<sup>2</sup>. The attractive, qualitative, intelligent functional materials, components and systems are designed by new material nanotechnology technique<sup>3-4</sup>. Superior physical properties of ferrites like recording are used for magnetic resonance imaging enhancement, catalysis, and sensors<sup>5</sup>. The  $\text{MFe}_2\text{O}_4$  is the chemical formula of spinel ferrites where M is divalent metal cations<sup>6</sup>. Magnesium ferrite ( $\text{MgFe}_2\text{O}_4$ ) has an inverse spinel structure in which  $\text{Mg}^{2+}$  cations are on octahedral sites and zinc ferrite ( $\text{ZnFe}_2\text{O}_4$ ) has normal spinel structure in which  $\text{Zn}^{2+}$  cations occupy tetrahedral sites<sup>7-10</sup>. The intensive properties of the small scale size spinel ferrites were used for biomedical applications<sup>11-13</sup>. The co-precipitation, hydrothermal, sol-gel, etc techniques were used to produce high quality nanoparticle and particle size in the range between 2 to 100 nm<sup>14-15</sup>.

In this work,  $\text{Ni}_{0.4}\text{Mg}_{0.4}\text{Cd}_{0.2}\text{Y}_y\text{Fe}_{2-y}\text{O}_4$  Nanoferrites (where  $y = 0.025$  to  $0.125$ ) were synthesized using co-precipitation methods. X-ray diffraction (XRD) was used in order to investigate the structural of  $\text{Y}^{3+}$  substituted nickel-magnesium-cadmium nano-ferrites and to determine the lattice parameters and the space group symmetry. Ultraviolet visible spectrometer (UV-Vis) and Fourier Transform Infrared Spectroscopy (FTIR) were used to

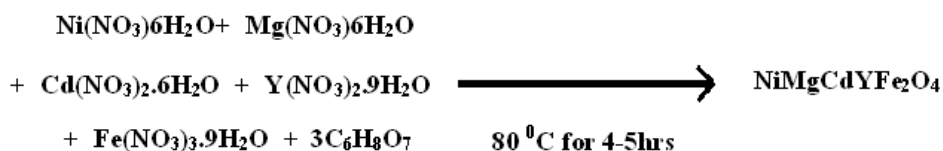
investigate the optical properties of crystallite nanoparticles.

## MATERIAL AND METHOD

The  $Y^{3+}$  doped in Ni-Mg-Cd ferrite powders were synthesized by sol-gel autocombustion method at low temperatures for different compositions of  $Ni_{0.4}Mg_{0.4}Cd_{0.2}Y_yFe_{2-y}O_4$  (where  $y = 0.025, 0.050, 0.075, 0.100$  and  $0.125$ ). According to respective molar amounts of yttrium nitrate, magnesium nitrate, nickel nitrate, cadmium nitrate, ferric nitrate of AR grade with 99% purity and citric acid as a fuel were used with stoichiometric ratio (1:3) proportion to obtain the final product<sup>16</sup>. All these chemicals were dissolved in double distilled water and stirred till to obtain the homogeneous solution. Ammonium hydroxide was added drop by drop to maintain pH between 7 to 8 during the stirring process and solution was continuously stirred with 80-100 °C for about 4-5 hours to obtain sol. After 4-5 hours, gel converts into ash and ash convert into powder. Finally get fine powder of  $Ni_{0.4}Mg_{0.4}Cd_{0.2}Y_yFe_{2-y}O_4$  ferrite nanoparticles after auto combustion. The powder was sintered at 400 °C for 2 hours.

The X-ray diffractometer (Cu-K $\alpha$  radiation of wavelength 1.54 Å at 40 kV) were performed a scanning 20 to 80 degree with step of 0.02 degree per second for each prepared sample to study structural characterization and used to determine lattice parameter with grain size. The optical characteristics was studied using Fourier Transformation Infrared spectroscopy (FT-IR) of Bruker 3000 Hyperion microscope with vertex 80 single point detector performing images resolution ranging between 7500 to 450 cm<sup>-1</sup> and UV-Visible spectroscopy. Further investigations of the optical properties are under way to elucidate the effective role of inter particle interactions in these samples.

The general chemical reaction of the synthesis sample is as follows;



## 3. RESULTS AND DISCUSSIONS

### 3.1 Structural Studies

**XRD Analysis:** The prepared powders of  $Y^{3+}$  doped Ni-Mg-Cd nanoferrite were characterized by X-ray diffraction and pattern of sintered powder is shown in figure-1. The XRD pattern conform the formation of a homogeneous spinel cubic structure and the broad peaks indicates fine particle nature of the nanoparticles. Scherer's formula was used to determine the particle (grain) size.

$$t = \frac{0.9\lambda}{\beta \cos \theta} \quad (1)$$

Where, ' $\lambda$ ' is wavelength of x-ray,

' $\theta$ ' is peak position, and

' $\beta$ ' is FWHM of the peak position.

The average particle (grain) size of nanoparticles was noted in table-1 and it is ranging between 17 to 25 nm. This indicates if the concentration of  $Y^{3+}$  doped increases then average particle size decreases. Lattice parameters were

calculated for sintered sample is ranging from 1.9228 to 2.1300 Å<sup>0</sup>. The value of lattice constant of Ni-Mg-Cd ferrite shows the expansion of unit cell with rare earth yttrium doping when compared with pure yttrium ferrite and the deviation in lattice parameter attributed to the cations rearrangement in the nanosize prepared ferrites. The Y<sup>3+</sup> substituted ferrites have high stability relative to Ni-Mg-Cd ferrite due to doping of large ionic radius of Y<sup>3+</sup> ions (0.9 Å<sup>0</sup>) with small ionic radius Fe<sup>3+</sup> ions (0.645 Å<sup>0</sup>).

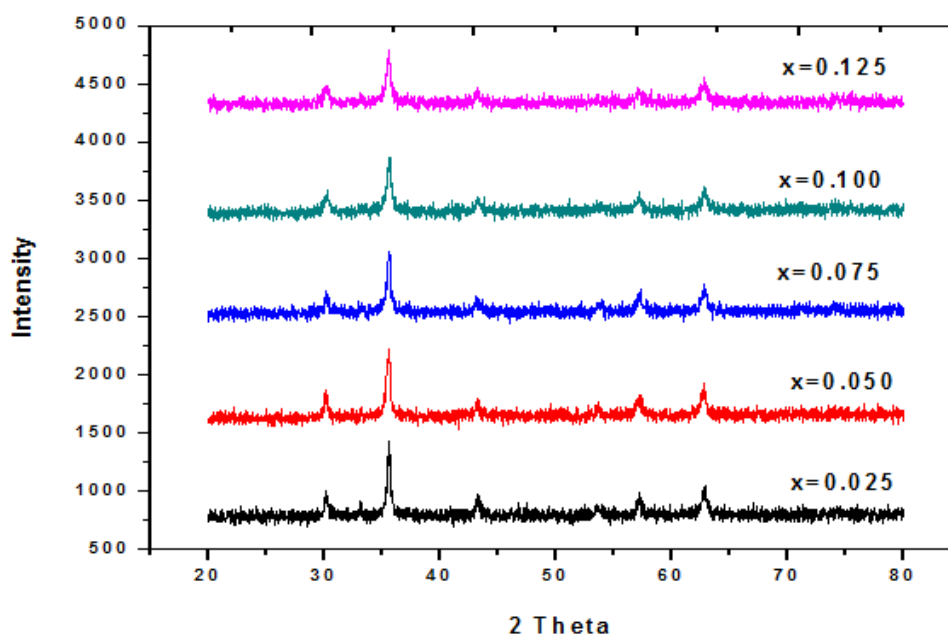


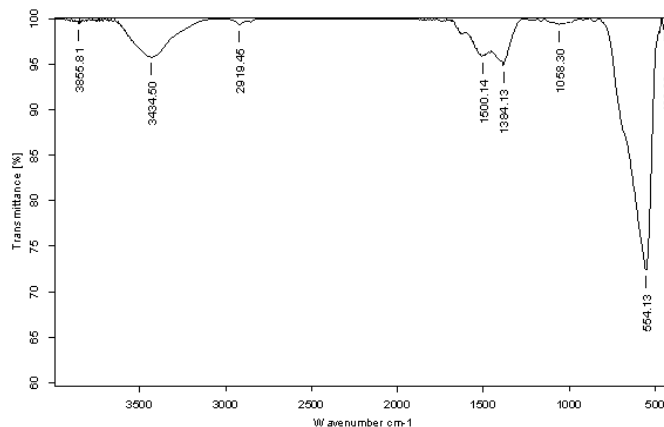
Figure 1: X-ray Diffraction Pattern of Ni<sub>0.4</sub>Mg<sub>0.4</sub>Cd<sub>0.2</sub>Y<sub>y</sub>Fe<sub>2-y</sub>O<sub>4</sub>

Table 1: The Grain Size of Prepared Samples Ni<sub>0.4</sub>Mg<sub>0.4</sub>Cd<sub>0.2</sub>Y<sub>y</sub>Fe<sub>2-y</sub>O<sub>4</sub> by x-Ray Diffraction

Obs. No.	Composition	Grain size (t) nm	Lattice constant (a) Å <sup>0</sup>
1	y = 0.025	23	2.1309
2	y = 0.050	25	2.1338
3	y = 0.075	21	2.1305
4	y = 0.100	22	2.1300
5	y = 0.125	17	1.9228

## Optical Studies

**FTIR Analysis:** In order to investigate the chemical functional groups on the synthesized Ni<sub>0.4</sub>Mg<sub>0.4</sub>Cd<sub>0.2</sub>Y<sub>y</sub>Fe<sub>2-y</sub>O<sub>4</sub>, FTIR spectroscopy are performed. The FTIR spectra of the prepared Ni<sub>0.4</sub>Mg<sub>0.4</sub>Cd<sub>0.2</sub>Y<sub>0.100</sub>Fe<sub>1.900</sub>O<sub>4</sub> are shown in figure 2 to know the bonding characteristics of the materials. The peaks at 429.68 cm<sup>-1</sup> and 554.13 cm<sup>-1</sup> are the peaks of Fe-O bond in Y doped Ni-Mg-Cd ferrite and it is arises due to the lattice vibrations of the oxide ions against cations. The peak at 1384.13 cm<sup>-1</sup> indicates the presence of O-H bond due to bending vibration. The broad peak at 3434.50 cm<sup>-1</sup> gives presence of hydroxyl group in the material and indicates that the material absorbed moisture from atmosphere during analysis.



**Figure 2(a): FT-IR Spectrum of  $\text{Ni}_{0.4}\text{Mg}_{0.4}\text{Cd}_{0.2}\text{Y}_{0.100}\text{Fe}_{1.900}\text{O}_4$**

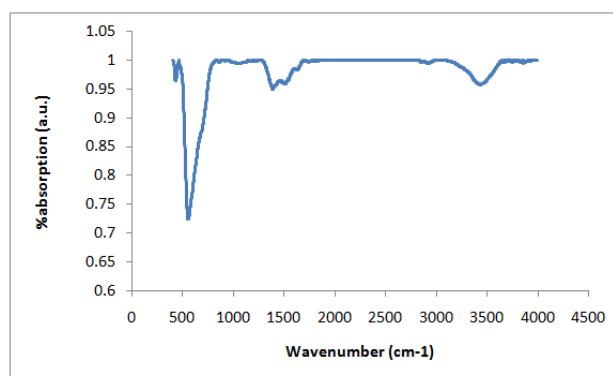


**Figure 2(b): Absorption Spectra of  $\text{Ni}_{0.4}\text{Mg}_{0.4}\text{Cd}_{0.2}\text{Y}_{0.100}\text{Fe}_{1.900}\text{O}_4$**

The intense absorption bond is observed at  $554.13\text{ cm}^{-1}$  which shows the characteristic bond of spinel structure which may due to presence of Fe-O and Y-O bonds or crystalline nature of Y doped Ni-Mg-Cd ferrite. Hence, FT-IR analysis supports the observation of XRD analysis and confirms the crystalline nature of ferrite. So, the peaks at  $476\text{ cm}^{-1}$  and  $1058\text{ cm}^{-1}$  confirms the presence of yttrium doped in Ni-Mg-Cd ferrite. Finally, the doping of  $\text{Y}^{3+}$  on Ni-Mg-Cd ferrite was confirmed by different pattern of the plots and the difference in relative position and intensity of the peaks appeared in the FT-IR plots of the prepared samples. This indicates normal ferromagnetic materials.

**UV-Visible Analysis:** The figure-3 shows optical properties were studied from UV-Visible spectroscopy to calculate the band gap energy. In the absorption molecules of non-bonding electrons can absorb the energy in the form of ultraviolet or visible light to excite this electron to higher or anti-bonding molecular orbit. The energy band gap was calculated for samples with different ratio using following formula;

$$E = \frac{h c}{\lambda} \quad (2)$$

Energy band gap was found to be 3.9935, 4.0390, 4.0655, 4.1196 and 4.1541 eV. The substitution was resulted in slight increase in the lattice constant and that sequentially may lead to the slightly decrease in the energy gap. The average Band gap of prepared sample is 4.0743 eV and wavelength absorb by 508 nm. It is in the range of semiconductor materials.

Table 2: The Band Gap Energy of  $\text{Ni}_{0.4}\text{Mg}_{0.4}\text{Cd}_{0.2}\text{Y}_y\text{Fe}_{2-y}\text{O}_4$  by UV-Visible Spectroscopy

Obs. No.	Composition	Wavelength (nm)	Band gap energy (eV)
1	y=0.025	310.5	3.9935
2	y=0.050	307.0	4.0390
3	y=0.075	305.0	4.0655
4	y=0.100	301.0	4.1196
5	y=0.125	298.5	4.1541

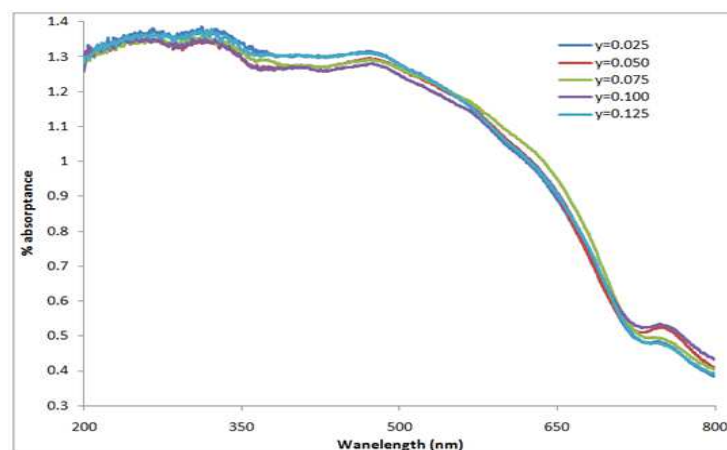


Figure 3: UV-Visible Spectra of  $\text{Ni}_{0.4}\text{Mg}_{0.4}\text{Cd}_{0.2}\text{Y}_y\text{Fe}_{2-y}\text{O}_4$

## CONCLUSIONS

The  $\text{Ni}_{0.4}\text{Mg}_{0.4}\text{Cd}_{0.2}\text{Y}_y\text{Fe}_{2-y}\text{O}_4$  nanoferrites were synthesized using sol-gel autocombustion technique. The increase in the  $\text{Y}^{3+}$  concentration gives the significant changes in the particle size and optical properties of the composition  $\text{Ni}_{0.4}\text{Mg}_{0.4}\text{Cd}_{0.2}\text{Y}_y\text{Fe}_{2-y}\text{O}_4$  (where  $y = 0.025, 0.050, 0.075, 0.100$  and  $0.125$ ). The FT-IR spectroscopy study shows two main metal oxygen bands in the range of  $429.68$  to  $554.13\text{ cm}^{-1}$  confirms the formation of cubic spinel phase structure of  $\text{Y}^{3+}$  substitute in Ni-Mg-Cd ferrite. The synthesis of nanoparticles with crystalline size decreases and lattice constant increases as the concentration increases and is in the range of  $17$  to  $25\text{ nm}$  for  $400^\circ\text{C}$ . The UV-Visible analysis shows band gap energy increases with increase in  $\text{Y}^{3+}$  concentration. The UV-Visible study shows average Band gap energy is  $4.0743\text{ eV}$  and wavelength absorb by  $508\text{ nm}$ . This result prepared ferrite materials is in the range of semiconductor materials.

## ACKNOWLEDGEMENTS

The authors are thankful to IIT, Powai (Mumbai), Savitribai Phule Pune University, Abasaheb Garware, College, Pune and PDE's Baburaoji Gholap College, New Sangavi, Pune, India for providing the instrumental facilities for the characterization purpose.

## REFERENCES

1. Flores-Acosta, M., Sotelo-Lerma, M., Arizpe-Chavez, H., Castillon-Barraza, F.F. and Ramirez-Bon, R.J. (2003) Excitonic Absorption of Spherical PbS Nanoparticles in Zeolite A. *Solid State Communications*, **128**, 407-411. <http://dx.doi.org/10.1016/j.ssc.2003.09.008>
2. Pulisova, P., Kovac, J., Voigt, A. and Raschman, P. (2013) Structure and Magnetic Properties of Co and Ni Nano-Ferrites Prepared by a Two Step Direct Microemulsions Synthesis. *Journal of Magnetism and Magnetic Materials*, **341**, 93-99. <http://dx.doi.org/10.1016/j.jmmm.2013.04.003>

3. Lodhi, M.Y., Mahmood, K., Mahmood, A., Malika, H., Warsi, M.F., Shakir, I., Asghar, M. and Khan, M.A. (2014) New  $Mg_{0.5}Co_xZn_{0.5-x}Fe_2O_4$  Nano-Ferrites: Structural Elucidation and Electromagnetic Behavior Evaluation. *Current Applied Physics*, **14**, 716-720. <http://dx.doi.org/10.1016/j.cap.2014.02.021>
4. Jan, L.S., Radiman, S., Siddig, M.A., Muniandy, S.V., Hamid, M.A. and Jamali, H.D. (2004) Preparation of Nanoparticles of Polystyrene and Polyaniline by  $\gamma$ -Irradiation in Lyotropic Liquid Crystal. *Colloids and Surfaces A: Physicochemical and Engineering Aspects*, **251**, 43-52. <http://dx.doi.org/10.1016/j.colsurfa.2004.09.025>
5. Mathew, D.S. and Juaug, R.-S. (2007) An Overview of the Structure and Magnetism of Spinel Ferrite Nanoparticles and Their Synthesis in Micro Emulsions. *Chemical Engineering Journal*, **129**, 51-65. <http://dx.doi.org/10.1016/j.cej.2006.11.001>
6. Rahman, S., Nadeem, K., Anis-ur-Rehman, M., Mumtaz, M., Naeem, S. and Letofsky-Papst, I. (2013) Structural and Magnetic Properties of ZnMg-Ferrite Nanoparticles Prepared Using the Co-Precipitation Method. *Ceramics International*, **39**, 5235-5239. <http://dx.doi.org/10.1016/j.ceramint.2012.12.023>
7. Pradeep, A., Priyadharsini, P. and Chandrasekaran, G. (2008) Sol-Gel Route of Synthesis of Nanoparticles of  $MgFe_2O_4$  and XRD, FTIR and VSM Study. *Journal of Magnetism and Magnetic Materials*, **320**, 2774-2779. <http://dx.doi.org/10.1016/j.jmmm.2008.06.012>
8. Greenwood, N.N. and Earnshaw, A. (1984) *Chemistry of the Elements*; Pergamon Press Ltd., Oxford, 279.
9. Ichiyanagi, Y., Kubota, M., Moritake, S., Kanazawa, Y., Yamada, T. and Uehashi, T. (2007) Magnetic Properties of Mg-Ferrite Nanoparticles. *Journal of Magnetism and Magnetic Materials*, **310**, 2378-2380. <http://dx.doi.org/10.1016/j.jmmm.2006.10.737>
10. Thummer, K.P., Chhantbar, M.C., Modi, K.B., Baldha, G.J. and Joshi, H.H. (2004) Localized Canted Spin Behaviour in  $Zn_xMg_{1.5-x}Mn_{0.5}Fe_2O_4$  Spinel Ferrite System. *Journal of Magnetism and Magnetic Materials*, **280**, 23-30. <http://dx.doi.org/10.1016/j.jmmm.2004.02.017>
11. Kumara, C.S.S.R. and Mohammad, F. (2011) Magnetic Nanomaterials for Hyperthermia-Based Therapy and Controlled Drug Delivery. *Advanced Drug Delivery Reviews*, **63**, 789-808. <http://dx.doi.org/10.1016/j.addr.2011.03.008>
12. Giri, J., Pradhan, P., Somani, V., Chelawat, H., Chhatre, S., Banerjee, R. and Bahadur, D. (2008) Synthesis and Characterizations of Water-Based Ferrofluids of Substituted Ferrites [ $Fe_{1-x}B_xFe_2O_4$ ,  $B=Mn, Co$  ( $x=0-1$ )] for Biomedical Applications. *Journal of Magnetism and Magnetic Materials*, **320**, 724-730. <http://dx.doi.org/10.1016/j.jmmm.2007.08.010>
13. Sharifi, I., Shokrollahi, H. and Amiri, S. (2012) Ferrite-Based Magnetic Nanofluids Used in Hyperthermia Applications. *Journal of Magnetism and Magnetic Materials*, **324**, 903-915. <http://dx.doi.org/10.1016/j.jmmm.2011.10.017>
14. Chen, Y., Ruan, M., Jiang, Y.F., Cheng, S.G. and Li, W. (2010) The Synthesis and Thermal Effect of  $CoFe_2O_4$  Nanoparticles. *Journal of Alloys and Compounds*, **493**, L36-L38. <http://dx.doi.org/10.1016/j.jallcom.2009.12.170>
15. Liu, Q., Sun, J.H., Long, H.R., Sun, X.Q., Zhong, X.J. and Xu, Z. (2008) Hydrothermal Synthesis of  $CoFe_2O_4$  Nanoplatelets and Nanoparticles. *Materials Chemistry and Physics*, **108**, 269-273. <http://dx.doi.org/10.1016/j.matchemphys.2007.09.035>
16. Bhise, R.B. and Rathod, S.M. June (2016) Synthesis of Nanosized  $Y^{3+}$  Doped Ni-Mg-Cd Ferrite Powders and their Structural, Magnetic properties by Sol-gel Auto Combustion Method. *Res. J. Material Sci.*, Vol. 4(5), 1-4. E-ISSN 2320-6055